Wideband Millimeter-Wave Balun-Diplexer Based on a Novel Coupled Marchand Architecture for Compact Footprint and Phased-Array

Microwave and Optical Technology Letters

WILEY

RESEARCH ARTICLE OPEN ACCESS

Wideband Millimeter-Wave Balun-Diplexer Based on a Novel Coupled Marchand Architecture for Compact Footprint and Phased-Array Integration

Teanette van der Spuy[1,2] | Rob Maaskant[1] | Sten E. Gunnarson[3] | Henrik Holter[4] | Lukas Nyström[2]

[1]Electrical Engineering, Chalmers University of Technology, Gothenburg, Sweden | [2]Research and Development, Satcube AB, Gothenburg, Sweden | [3]Surveillance, SAAB, Järfälla, Sweden | [4]Hardware Research, Ericsson, Stockholm, Sweden

Correspondence: Teanette van der Spuy (teanette@chalmers.se)

Received: 28 July 2025 | **Revised:** 14 October 2025 | **Accepted:** 28 October 2025

Funding: This study is supported by the Swedish Foundation for Strategic Research (SERENA project), and the Advanced Digitalization program at the WiTECH center (DIGIARRAY project), financed by VINNOVA, Ericsson, Saab, Satcube, and Chalmers University of Technology.

Keywords: balun-diplexer | full-duplex | phased array | SatCom | shared aperture

ABSTRACT

This letter presents the first reported wideband balun-diplexer for mm-wave applications, designed for shared-aperture full-duplex array systems. By integrating balun and diplexer functionalities in a single component, we enable per-element self-interference suppression, while also facilitating the interface between the balanced feed of the antenna and the unbalanced ports found in many beamformer chips. A novel coupled Marchand topology enables a compact footprint compatible with the strict lattice constraints of grating-lobe-free phased arrays, and facilitates integration with the multilayer stackups commonly used in phased-array systems. The component targets K/Ka-band SatCom applications, with two 3.5-GHz-wide bands centered at 19 and 29 GHz, respectively. Fabricated on a Megtron 6 substrate, the prototype achieves a minimum TX–RX isolation of 20 dB, insertion losses of 1.5 and 2.3 dB in the lower/higher bands, respectively, and a common-mode rejection ratio exceeding 19 dB in both bands. The results confirm the feasibility of the proposed concept and demonstrate the first realization of a compact, mm-wave balun-diplexer for high-frequency phased-array integration.

1 | Introduction

The development of 5G and 6G networks demands compact antennas and highly integrated front-end architectures for mm-wave operation [1–4]. A promising approach for frequency-division duplexing systems, such as SatCom, cellular base stations, or wireless backhaul nodes, is the use of shared-aperture full-duplex array (SAFDA) antennas [4–7]. This approach offers a significant size advantage over dual-aperture antennas, but comes with increased self-interference (SI).

Traditionally, SAFDA systems have been realized by using diplexers to suppress the SI between the receive (RX) and transmit (TX) chains. This is particularly effective for fixed-beam systems, where a single (large) diplexer is connected to a corporate feed network [8–10]. However, in phased-array systems, where beamformer integrated circuits (BFICs) operate at each antenna element, SI suppression must be implemented on a per-element basis [4]. This imposes strict constraints on the size of diplexer circuitry, which must fit within the array's lattice spacing, typically $0.5\lambda \times 0.5\lambda$ at the highest operating frequency.

Abbreviations: BFIC, beamformer integrated circuit; NTN, nonterrestrial networks; OC, open circuit; RX, receive; SAFDA, shared-aperture full-duplex array; SC, short circuit; SI, self-interference; TX, transmit; UT, user terminal.

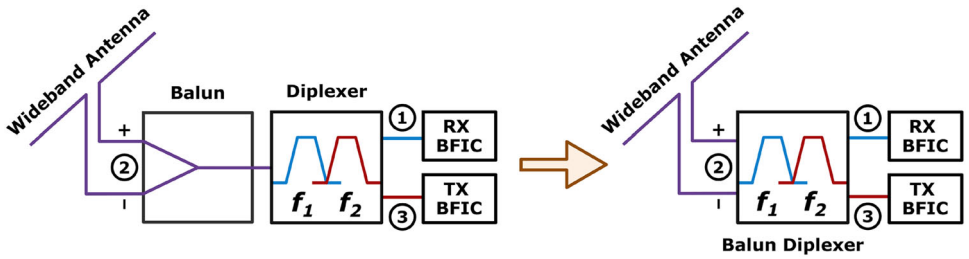

FIGURE 1 | Proposed architecture of the SAFDA element. BFIC, beamformer integrated circuit; RX, receive; SAFDA, shared-aperture full-duplex array; TX, transmit.

Furthermore, many SAFDA antenna elements utilize balanced feeds, which provide high immunity to noise interference, and reduce undesired parasitic coupling in the feed network. Differential feeding also improves polarization purity in the radiating element, which is critical for several key 6G applications, such as nonterrestrial networks. In contrast, most of the current commercial mm-wave BFICs (from Anokiwave, Renesas, Sivers, Analog Devices, Ensilica) provide unbalanced signals, which require a balun to interface with the antenna elements.

As the demand for these technologies in the mm-wave spectrum increases, the need for high system integration becomes critical—particularly for SAFDA systems, where beamsteering antenna physics results in strict lattice spacing constraints. This creates a need for innovative design solutions to combine the functionality of the diplexer and balun components within a limited physical footprint [4] (Figure 1).

In recent years, several works have reported the balun-diplexers in highly compact configurations [2, 11–20]. However, these designs make use of either microstrip [2, 11–19] or on-chip [20] technology, which is not suitable for integration with SAFDA systems, where the outer layers of the stackup are typically reserved for the BFIC network and the antenna aperture. Furthermore, most of these designs operate in the sub-6 GHz range, with miniaturization techniques that do not scale well with frequency.

To address these limitations, we present a novel mm-wave balun-diplexer that combines compact size, wideband performance, and integration compatibility with multilayer SAFDA architectures. The design uses two superimposed coupled Marchand baluns to realize both diplexing and balun functionalities in a small footprint. This approach supports full-duplex operation at K/Ka-band frequencies and is validated for SatCom user terminal (UT) applications, which impose stringent constraints on size, weight, and cost. The *primary innovations* of this study are as follows:

- a *mm-wave balun-diplexer* with a *compact footprint* that conforms to the lattice spacing of a K/Ka-band SatCom SAFDA system, realized through;
- a *novel architecture* that consists of dual-stacked cross-coupled Marchand baluns, enabling stripline-based multilayer integration;
- demonstration of *wideband performance* in SatCom RX/TX bands.

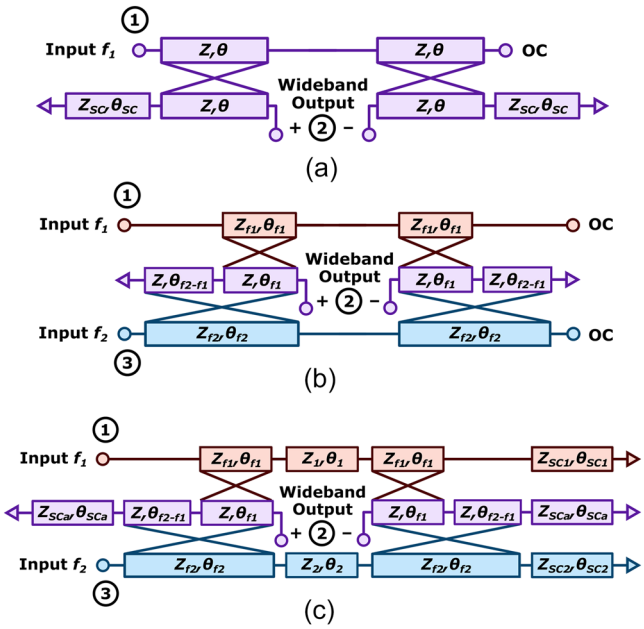

FIGURE 2 | Development of the balun-diplexer ("red: high frequency, blue: low frequency"). (a) Classic Marchand architecture, (b) Proposed balun-diplexer architecture, and (c) Modified architecture for SAFDA applications. OC, open circuit; SAFDA, shared-aperture full-duplex array.

The paper is structured as follows: Section 2 outlines the principle of operation, the proposed architecture, and the design constraints, goals, and procedure. The simulated and measured design validation is shown in Section 3, as well as a comparison with state-of-the-art (SOTA) designs, followed by the conclusion in Section 4.

2 | Balun-Diplexer Design

2.1 | Principle of Operation

The classic Marchand balun consists of two cascaded 90° couplers, with short circuit (SC) and open circuit (OC) terminations, as shown in Figure 2a [21, 22]. The reflected waves from these stubs combine constructively at the balanced port, producing a broadband differential output. For identical 3 dB couplers and electrically short reflective stubs, this architecture can realize components with fractional bandwidths of 74%–114% [23–25]. The SC stub lengths, however, strongly influence the phase of the

reflected waves and can thus be adjusted to shape or limit the operational bandwidth, as shown in Figure 3.

This provides a mechanism for embedding diplexing behavior into the balun structure: by extending the SC lines, a secondary set of 90° couplers can be superimposed. This forms a second, lower-frequency Marchand balun that shares part of its structure with the higher-frequency one, as shown schematically in Figure 2b. The result is a dual-band configuration in which two Marchand baluns are implemented using only three coupled layers: one operating at high frequency (red), one operating at low frequency (blue), and a shared structure which operates in both frequency bands (purple).

Together, these layers realize simultaneous balun and diplexer functionality. Ideally, the high- and low-frequency paths are electromagnetically isolated, with only the shared layer mediating coupling. In practice, some residual interaction between the two frequency paths remains. However, this can be partially addressed by choosing the OC stub lengths so that the unwanted signal from one path experiences destructive interference at the other path's input port. In this way, the same interference and reflection mechanisms that establish the balun's balanced output are leveraged to create frequency-selective cancellation, and the diplexing and balun functionalities are combined within a compact Marchand-based network.

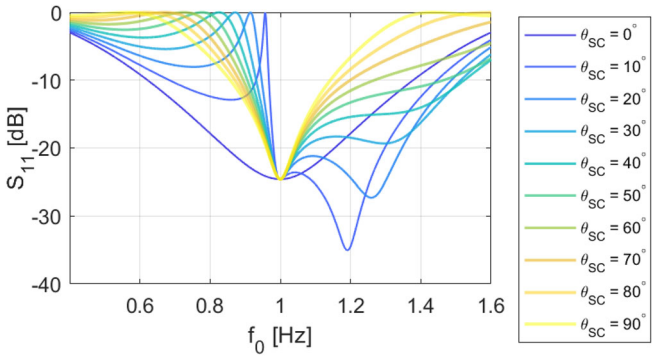

FIGURE 3 | Marchand balun bandwidth for different SC line lengths. SC, short circuit.

2.2 | Architecture and Constraints

As described in Section 2.1, we propose a novel architecture of dual-stacked cross-coupled Marchand baluns that integrates balun and diplexing functions (Figure 2b). The challenge with this topology is fitting the lower-band 90° couplers within a lattice spacing of $0.5\lambda_{HF} \times 0.5\lambda_{HF}$, where λ_{HF} is the free-space wavelength of the highest frequency of operation. This lattice is required for SAFDA systems targeting grating-lobe-free scanning up to 60°, such as SatCom UTs. Within this limited area, conventional edge-coupled implementations fail to provide sufficient coupling at mm-wave frequencies, since the coupling coefficient decreases rapidly with frequency as conductor spacing becomes constrained by fabrication tolerances. Instead, we propose the use of broadside coupled striplines for the 90° couplers, resulting in a triple-layer structure as shown in Figure 4b. This maximizes coupled power transfer by increasing the electric field overlap between the coupled lines while maintaining low dielectric loss in the Megtron 6 substrate. Not only does this inherently reduce insertion loss, it also provides a more controllable coupling coefficient, while maintaining a compact footprint. Furthermore, it introduces physical distance between the two input layers, which increases isolation between these ports and improves diplexing functionality.

A further challenge to consider in highly integrated SAFDA systems is the potential to couple power to neighboring components—particularly since Marchand baluns employ OC stubs in close proximity to adjacent unit cells. To avoid this, we replace them with SC stubs, appropriately transformed with quarter-wavelength impedance converters, as shown in Figure 2c. This figure also includes practical line lengths between the respective couplers, θ_1, θ_2.

Lastly, to achieve a good common-mode rejection ratio (CMRR), which is important for the balun functionality, the design should be symmetric. However, some asymmetries are introduced in the design for diplexing functionality: the lengths of the SC and OC stubs are altered to improve the isolation between the unbalanced ports, and the widths of the stripline sections are altered for impedance matching. This trade-off between balun and diplexing functionality should be carefully considered for the chosen application, and symmetry should be maintained in the design as far as possible.

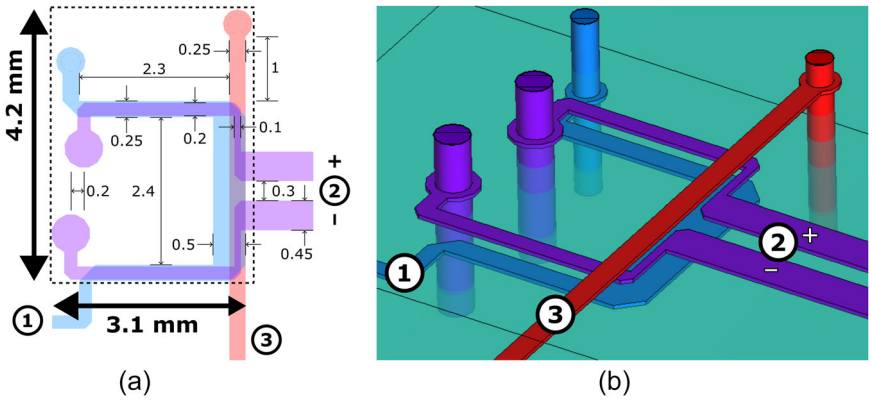

FIGURE 4 | Multilayer stripline layout of the balun-diplexer. (a) Top view and (b) perspective view.

2.3 | Design Goals

The operational bandwidth for K/Ka-band SatCom UTs is

- 17.7–21.2 GHz for the RX band,
- 27.5–31.0 GHz for the TX band.

To avoid grating lobes over the entire scan volume over these bands, the footprint of the balun-diplexer must fit in the appropriate array lattice spacing of 4.8 mm × 4.8 mm. Furthermore, the works in [26, 27] suggest that a diplexer isolation of ≥ 10 dB is sufficient for Ku-band SAFDA systems for SatCom operation. This should also be sufficient for the K/Ka-band case, where the bands of operation are further apart, and the TX and RX chains have more inherent isolation.

In terms of balun functionality, a good CMRR translates into a good polarization purity of the SAFDA. However, polarization purity can also be improved through beamforming schemes [28]. Therefore, a CMRR of ≥20 dB is considered sufficient for this design. Lastly, an insertion loss of 1–2 dB is common among balun-diplexers. This should be evaluated against a good isolation level, as the work in [26, 27] shows a clear trade-off between system gain and achieved isolation.

2.4 | Design Procedure

Initial line lengths were chosen for the center frequencies of the operational bands: $\theta_{f1} = \theta_{SC1} = 90°$ at 19.45 GHz, $\theta_{f2} = \theta_{SC2} = 90°$ at 29.25 GHz, and $\theta = 90°$ at 25 GHz (between the TX and RX bands). Thereafter the impedances and remaining line lengths ($\theta_{SCa}, \theta_{SCb}$), were optimized using the full-wave EM simulator CST Studio Suite 2023[1] to achieve the specified insertion loss, CMRR, and isolation. The resulting triple-layer stripline structure is shown in Figure 4. From this figure, it is clear that there is additional potential for miniaturization if the coupled line sections are meandered. However, the current component footprint design fulfills the design goal, and is therefore left unaltered in favor of simplicity.

3 | Design Verification

3.1 | Fabrication and Measurements

The component was fabricated on a seven-layer Megtron 6 stackup. Solderless 2.92 mm Southwest end-launch connectors were used to interface with the device under test (DUT), and a custom multiline through-reflect-line calibration kit was used to de-embed the effects of the measuring cables and connectors. The DUT connected to a four-port Vector network analyzer is shown in Figure 5.

Measured and simulated results are compared in Figures 6 (transmission coefficients) and 7 (reflection coefficients). The transmission coefficients show excellent agreement between measurement and simulation. However, while overall agreement is good in the reflection coefficients, a reflection-induced ripple is observed in the measured results for ports 1 and 3.

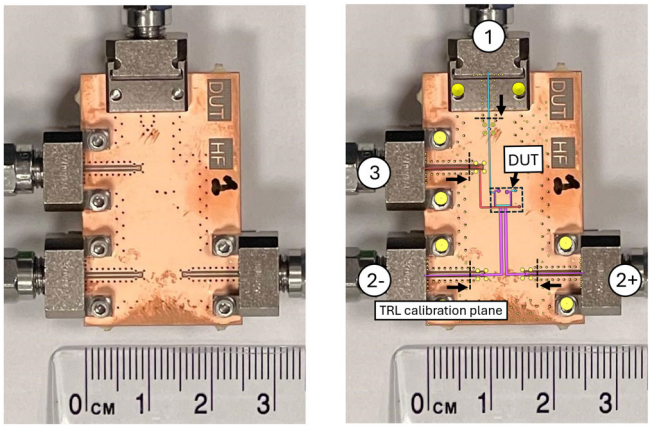

FIGURE 5 | DUT with (right) and without (left) the stripline design. DUT, device under test; TRL, through-reflect-line.

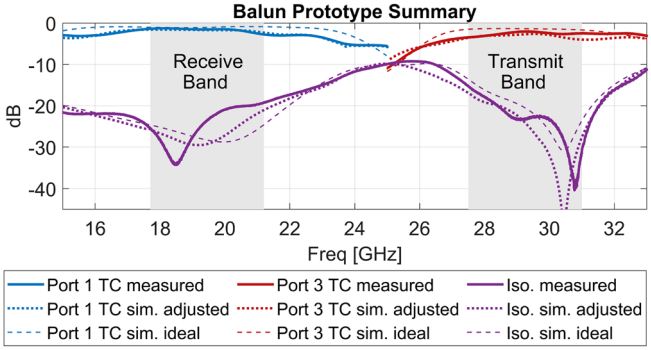

FIGURE 6 | Transmission coefficient (TC, defined as $|S_{2x}|$, where $x \in \{1, 3\}$) and isolation ($|S_{31}|$) of the device under test.

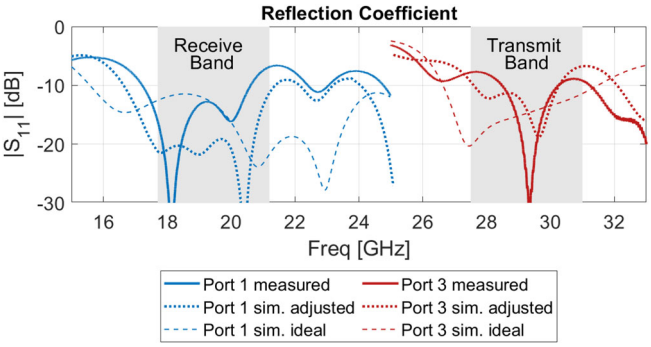

FIGURE 7 | Reflection coefficient of the unbalanced ports.

Assuming accurate calibration to the microstrip feed lines and a reflection originating at the first via transition at port 1, the ripple suggests an additional reflection approximately 30 mm from the via, which aligns exactly with the via fence at the opposite printed circuit board edge. This indicates a standing wave that is trapped between the port and the opposing via fence, which both degrades the reflection coefficient and contributes to the overall insertion loss of the component. Changing the via spacing and placement in simulation yields the adjusted simulation results in Figures 6 and 7, which show improved agreement with the measurements. In future work, the via fence will be included explicitly in the EM optimization process to improve the performance.

TABLE 1 | Comparison with state-of-the-art and lower/upper band.

	Design parameters			Performance metrics				
Technology	**Ports**	**Size (λ^2_{HF})**	**Size (mm^2)**	**FBW (%)**	**IL (dB)**	**Iso. (dB)**	**CMRR (dB)**	**f_c (GHz)**
SL PCB [11]	B-U	0.40 × 0.34	97 × 82	7.5/8.0***	0.7/0.6	30/30	—	0.8/1.2
SL PCB [12]	B-U	0.35 × 0.17	20 × 10	4.1/3.6*	1.2/1.6	39/40	36/34	2.5/5.1
SL PCB [14]	B-U	0.70 × 0.35	78 × 40	11/8.0*	1.5/2.3	25/25	28/58	1.9/2.5
SL PCB [17]	B-U	0.65 × 0.46	35 × 25	9.3/5.7**	2.7/3.7	40/40	30/30	2.6/5.4
ML PCB [Sim]	**U-B**	**0.43 × 0.32**	**4.2 × 3.1**	**18/12*****	**1.0/1.4**	**20/15**	**19/22**	**19.0/29.0**
ML PCB [Meas]	**U-B**	**0.43 × 0.32**	**4.2 × 3.1**	**18/6.0*****	**1.5/2.3**	**20/20**	**19/22**	**19.0/29.0**

Note: λ_{HF}, free-space wavelength of the highest frequency of operation. Boldface is used to indicate that these are the results of the current work.
Abbreviations: B-U, balanced-to-unbalanced; CMRR, common-mode rejection ratio; FBW, fractional bandwidth, either 3dB*/1 dB** transmission or −10 dB*** reflection bandwidth; IL, insertion loss; Iso., isolation; Meas, measured; PCB, printed circuit board; Sim, simulated; SL/ML, single-/multilayer.

3.2 | Comparison With SOTA

The design is compared with the SOTA in Table 1. First, this is the only design to operate in the mm-wave spectrum—existing designs are all for sub-6 GHz applications. Furthermore, this study shows a significantly higher fractional bandwidth than the SOTA, while maintaining a compact footprint of less than $0.5\lambda_{HF} \times 0.5\lambda_{HF}$. This is achieved through the novel dual-stacked cross-coupled Marchand architecture, which provides wideband performance while exploiting the z-dimension to reduce the component footprint.

Although high-frequency, multilayer designs typically suffer from higher losses, our design remains remarkably comparable to the SOTA in terms of CMRR, isolation, and insertion loss. This is due to the broadside coupled lines, which maximize the coupled power transfer of the hybrids. There is potential to further improve the isolation performance through the addition of filtering stubs, though omitted here to illustrate the component's fundamental performance. The upper band bandwidth can also be improved with optimization of the via fence to reduce the interference ripples, as discussed in Section 2.

To the best of the authors' knowledge, this is the first design of its kind for mm-wave applications and the only one directly compatible with multilayer SAFDA stackups.

4 | Conclusion

In this study, a novel wideband balun-diplexer was introduced—the first of its kind for mm-wave systems—based on the superposition of two Marchand baluns, which is readily realizable through broadside-coupled striplines. The advantage of this configuration is its compactness and ease of integration with multilayer SAFDA systems. On the basis of this architecture, a component was designed and manufactured in multilayer stripline for the K/Ka-band SatCom use-case, which requires a fractional bandwidth of 18%/12% in the RX and TX bands, respectively. The measured results show a minimum isolation of 20 dB between the TX–RX bands, an insertion loss of 1.5 and 2.3 dB in the lower and higher bands, respectively, and a CMRR better than 19 dB in both bands. Furthermore, the measured and simulated results show good agreement, despite the presence of additional reflections at the component interfaces. These results demonstrate the feasibility of the proposed concept and highlight its potential for high-frequency full-duplex applications requiring compact, integrable front-end components.

Acknowledgments

The authors would also like to acknowledge discussions with the following individuals, contributing to the DigiArray project: Ashraf Uz Zaman and Mustafa Ayebe (Chalmers University of Technology), Thomas Schäfer (Satcube), Darwin Blanco (Ericsson), Johan Malmström, Andreas Wikström, and Magnus Isacsson (SAAB). This study is supported by the Swedish Foundation for Strategic Research (SERENA project), and the Advanced Digitalization program at the WiTECH center (DIGIARRAY project), financed by VINNOVA, Ericsson, Saab, Satcube, and Chalmers University of Technology.

Conflicts of Interest

The authors declare no conflicts of interest.

Data Availability Statement

The data that support the findings of this study are available from the corresponding author upon reasonable request.

Endnotes

[1] See https://www.3ds.com/products/simulia/cst-studio-suite.

References

1. Z. Shao and Y. P. Zhang, "Miniaturization of Differentially-Driven Microstrip Planar Inverted F Antenna," *IEEE Transactions on Antennas and Propagation* 67, no. 2 (2019): 1280–1283, https://doi.org/10.1109/TAP.2018.2883575.

2. J. Li, P. Hu, J. Chen, K. D. Xu, C. X. Mao, and X. Y. Zhang, "Dual-Polarized Duplex Base-Station Antenna With a Duplexer-Integrated Balun," *IEEE Antennas and Wireless Propagation Letters* 21, no. 2 (2022): 317–321, https://doi.org/10.1109/LAWP.2021.3130032.

3. T. Le Nadan, J. P. Coupez, S. Toutain, and C. Person, "Integration of an Antenna/Filter Device, using a Multi-Layer, Multi-Technology Process," in *1998 28th European Microwave Conference* (IEEE, 1998), Vol. 1, 672–677, https://doi.org/10.1109/EUMA.1998.338067.

4. K. Erkelenz, L. P. P. B. Bohl, A. Sieganschin, and A. F. Jacob, "A Compact K-/Ka-Band Rectangular-to-Coplanar Waveguide Transition

With Integrated Diplexer," *IEEE Microwave and Wireless Components Letters* 31, no. 6 (2021): 642–645, https://doi.org/10.1109/LMWC.2021.3064673.

5. J. Yin, H. Zhai, Y. Jia, et al., "High-Isolation Dual-Band Compact Duplex Array Based on Radiator-Shared System," *IEEE Antennas and Wireless Propagation Letters* 23, no. 7 (2024): 2056–2060, https://doi.org/10.1109/LAWP.2024.3378842.

6. A. H. Hussein, H. H. Abdullah, M. A. Attia, and A. M. Abada, "S-Band Compact Microstrip Full-Duplex Tx/Rx Patch Antenna With High Isolation," *IEEE Antennas and Wireless Propagation Letters* 18, no. 10 (2019): 2090–2094, https://doi.org/10.1109/LAWP.2019.2937769.

7. A. F. Jacob, T. Jaschke, and B. Rohrdantz, "Advanced Terminal Antenna Concepts for Mobile Satellite Communications," in *2018 Asia-Pacific Microwave Conference (APMC)* (IEEE, 2018), 252–254, https://doi.org/10.23919/APMC.2018.8617392.

8. A. Vosoogh, M. S. Sorkherizi, A. U. Zaman, J. Yang, and A. A. Kishk, "An Integrated Ka-Band Diplexer-Antenna Array Module Based on Gap Waveguide Technology With Simple Mechanical Assembly and No Electrical Contact Requirements," *IEEE Transactions on Microwave Theory and Techniques* 66, no. 2 (2018): 962–972, https://doi.org/10.1109/TMTT.2017.2757469.

9. Y. Zhou, H. Wei, J. Zhou, C. Cheng, and Y. Cheng, "Miniaturised High-Isolation K-/Ka-Band Diplexer With 3D Antarafacial Channel Integration Using Vertical Quasi-Coaxial Matching Network," *IET Microwaves, Antennas & Propagation* 18, no. 4 (2024): 291–296, https://doi.org/10.1049/mia2.12470.

10. C. Sanchez-Cabello, L. F. Herran, and E. Rajo-Iglesias, "Ka-Band Diplexer for 5G mmWave Applications in Inverted Microstrip Gap Waveguide Technology," *Electronics* 9, no. 12 (2020): 2094, https://doi.org/10.3390/electronics9122094.

11. C. F. Chen, Y. F. Tsai, B. H. Chen, R. Y. Yang, and Y. S. Zeng, "Integration Design of Compact Balun Filters and Duplexing Balun Filter With Arbitrary Frequency-Selective Response," *IEEE Access* 11 (2023): 141127–141136, https://doi.org/10.1109/ACCESS.2023.3342291.

12. H. Tian, H. Liu, S. Zheng, and T. Zuo, "Compact Filtering Balun-Diplexer Using Coupled-Line-Loaded Hairpin Ring Resonator," *IEEE Transactions on Circuits and Systems II: Express Briefs* 70, no. 3 (2023): 989–993, https://doi.org/10.1109/TCSII.2022.3220756.

13. F. Huang, J. Wang, L. Zhu, and W. Wu, "Compact Microstrip Balun Diplexer Using Stub-Loaded Dual-Mode Resonators," *Electronics Letters* 52, no. 24 (2016): 1994–1996, https://doi.org/10.1049/el.2016.3302.

14. Z. L. Wu, C. H. Lee, and H. H. Chen, "Balun Diplexer Design in Hybrid Structure of Microstrip Line and Slot-Line," in *2015 Asia-Pacific Microwave Conference (APMC)* (IEEE, 2015), Vol. 3, 1–3, https://doi.org/10.1109/APMC.2015.7413541.

15. J. Chen, J. Shen, N. Gao, and A. Zhang, "A Compact Balanced-to-Unbalanced Diplexer Using Interdigital Line Resonators," *Microwave Journal* 59, no. 4 (2016): 152.

16. J. Z. Chen, J. Shen, N. Gao, and J. Chen, "A Compact Balun-Diplexer Using Interdigital Line Resonators," *International Journal of RF and Microwave Computer-Aided Engineering* 25, no. 6 (2015): 485–489, https://doi.org/10.1002/mmce.20882.

17. C. M. Chen, S. J. Chang, C. F. Yang, and C. Y. Chen, "A Simple and Effective Method for Designing Frequency Adjustable Balun Diplexer With High Common-Mode Suppression," *IEEE Microwave and Wireless Components Letters* 25, no. 7 (2015): 433–435, https://doi.org/10.1109/LMWC.2015.2427583.

18. P. H. Wen, C. I. G. Hsu, C. H. Lee, and H. H. Chen, "Design of Balanced and Balun Diplexers Using Stepped-Impedance Slot-Line Resonators," *Journal of Electromagnetic Waves and Applications* 28, no. 6 (2014): 700–715, https://doi.org/10.1080/09205071.2014.885398.

19. C. H. Wu, C. H. Wang, and C. H. Chen, "A Novel Balanced-to-Unbalanced Diplexer Based on Four-Port Balanced-to-Balanced Bandpass Filter," in *2008 38th European Microwave Conference* (IEEE 2008), 28–31, https://doi.org/10.1109/EUMC.2008.4751378.

20. A. Güner, "Ka-Band Full Duplex System With Electrical Balance Duplexer for 5G Applications Using SiGe BiCMOS Technology" (master's thesis, Sabancı University, 2018).

21. G. Oltman, "The Compensated Balun," *IEEE Transactions on Microwave Theory and Techniques* 14, no. 3 (1966): 112–119, https://doi.org/10.1109/TMTT.1966.1126188.

22. J. Cloete, "Exact Design of the Marchand Balun," in *1979 9th European Microwave Conference* (IEEE 1979), 480–484, https://doi.org/10.1109/EUMA.1979.332751.

23. K. S. Ang and I. Robertson, "Analysis and Design of Impedance-Transforming Planar Marchand Baluns," *IEEE Transactions on Microwave Theory and Techniques* 49, no. 2 (2001): 402–406, https://doi.org/10.1109/22.903108.

24. Z. Y. Zhang, Y. X. Guo, L. Ong, and M. Chia, "A New Planar Marchand Balun," in *IEEE MTT-S International Microwave Symposium Digest* (IEEE 2005), 1207–1210, https://doi.org/10.1109/MWSYM.2005.1516893.

25. W. Feng and W. Che, "Ultra-Wideband Bandpass Filter Using Broadband Planar Marchand Balun," *Electronics Letters* 47 (2011): 198–199, https://doi.org/10.1049/el.2010.7282.

26. T. van der Spuy, R. Maaskant, M. Ivashina, L. Nyström, and T. Eriksson, "Self-Interference Suppression for SatCom Active Antenna Arrays Through Joint Transmit and Receive Beamforming," in *2024 18th European Conference on Antennas and Propagation (EuCAP)* (IEEE 2024), 1–5, https://doi.org/10.23919/EuCAP60739.2024.10501648.

27. T. van der Spuy, R. Maaskant, M. T. Behrens, M. Ivashina, and L. Nyström, "Out-of-band Interference Suppression of SatCom Antenna Arrays through Transmit Beamforming," in *2023 International Conference on Electromagnetics in Advanced Applications (ICEAA)* (IEEE 2023), https://doi.org/10.1109/ICEAA57318.2023.10297823.

28. K. F. Warnick, M. V. Ivashina, S. J. Wijnholds, and R. Maaskant, "Polarimetry With Phased Array Antennas: Theoretical Framework and Definitions," *IEEE Transactions on Antennas and Propagation* 60, no. 1 (2012): 184–196, https://doi.org/10.1109/TAP.2011.2167926.